IMMUNOMODULATION WITH SELF-CROSSLINKED POLYELECTROLYTE MULTILAYER BASED COATINGS

Helena Knopf-Marques[∞,¥], Sonali Singh[‡], Su Su Htwe[‡], Lucie Wolfova[Θ], Radovan Buffa [Θ], Jalal Bacharouche[ϕ], Grégory Francius[ϕ], Jean-Claude Voegel[∞,¥], Pierre Schaaf[∞,¥,⊥], Amir M. Ghaemmaghami[‡], Nihal Engin Vrana [∞,£], Philippe Lavalle [∞,¥*]

[∞]INSERM UMR 1121, 11 rue Humann, 67085 Strasbourg, France

[¥]Faculté de Chirurgie Dentaire, Fédération de Médecine Translationnelle de Strabourg, Université de Strasbourg, 3 rue Sainte Elisabeth, 67000 Strasbourg, France

[‡]Division of Immunology, School of Life Sciences, Faculty of Medicine and Life Sciences, University of Nottingham, Queen's Medics, al Centre, Nottingham, NG7 2UH, UK

[Θ] Contipro a.s., Dolni Dobrouc 401 561 02 Dolni Dobrouc, Czech Republic

[ϕ]Laboratoire de Chimie Physique et Microbiologie pour l'Environnement CNRS UMR7564, 405 rue de Vandoeuvre, 54600 Villers-les-Nancy, France

[⊥]Institut Charles Sadron, CNRS UPR 22, 23 rue du Lœss, 67034 Strasbourg, France

[£]Protip Medical, 8 Place de l'Hôpital, 67000 Strasbourg, France

*Corresponding Author: philippe.lavalle@inserm.fr

ABSTRACT. This study aims to design an optimal polyelectrolyte multilayer film of poly-L-lysine (PLL) and hyaluronic acid (HA) as an anti-inflammatory cytokine release system in order to decrease the implant failure due to any immune reactions. The chemical modification of the HA with aldehyde moieties allows self-crosslinking of the film and an improvement in the mechanical properties of the film. The crosslinking of the film and the release of immunomodulatory cytokine (IL-4) stimulate the differentiation of primary human monocytes seeded on the films into pro-healing macrophages phenotype. This induces the production of anti-inflammatory cytokines (IL1-RA and CCL18) and the decrease of pro-inflammatory cytokines secreted (IL-12, TNF-α and IL-1β). Moreover, we demonstrate that crosslinking PLL/HA film using HA-aldehyde is already effective by itself to limit inflammatory processes. Finally, this functionalized self-crosslinked PLL/HA-aldehyde films constitutes an innovative and efficient candidate for immunomodulation of any kind of implants of various architecture and properties.

Introduction

In recent years modification of biomaterial surfaces has been studied through various methods to render them bioactive. Surface coatings based on the layer-by-layer (LbL) method have been reported as a versatile and easy way of building polymeric surface coatings in environmentally friendly conditions, mostly from aqueous solutions.[1] The layer-by-layer method is based on the

electrostatic attraction between polyanions and polycations, the advantage of this method is the possibility of preparing ultra-thin and well-defined films.[2, 3] The spontaneous sequential adsorption of dissolved cationic and anionic polyelectrolytes on the substrate leads to the formation of ordered multilayer assemblies on the solid substrate surface.[4] These multilayers are widely used in biotechnology as controlled release systems, cell growth surfaces, anti-adhesive coatings and stimuli responsive surfaces. As the system is composed of charged molecules, it is ideal to control the release of charged bioactive agents such as cytokines and the strength of electrostatic interactions between the film and the cytokine should be a key parameter to determine the rate of release.[5, 6]

Biological properties and physicochemical characteristics of polyelectrolyte multilayer film coated device surfaces have been explored in order to get better properties between the implant and tissue interface.[7] The polyelectrolyte multilayer films PLL/HA ((poly(L-lysine) associated with hyaluronic acid) have been extensively studied. Furthermore, it has been successfully used for the release of growth factors and drugs.[8-11] Degradation of these films via dissolution is an obstacle for achieving long-term release of cytokines, which can be improved by structures crosslinking.[12, 13] Moreover, it is known that crosslinking these PLL/HA films strongly increase viability of cells growing on the films, mainly due to an increase of Young modulus.[14, 15] For example, the chemical crosslinking with a mixture of 1-ethyl-3-(3-dimethylaminopropyl)carbodiimide/N-hydroxysulfosuccinimide (EDC/NHS) is widely used for several polyelectrolyte multilayers (PEMs), typically, PLL/HA, PLL/polyglutamic acid (PLL/PGA), and chitosan/HA.[16-18] The EDC/NHS crosslinking involves a reaction between carboxylic groups of HA and amine groups of PLL. However, to achieve the crosslinking

reaction a long incubation time is required (at least 12 hours) and also some extensive rising steps after it, in order to eliminate excess products that can be toxic.[19]

Hyaluronic acid (HA) is a glycosaminoglycan mainly localized in extracellular matrix. It plays an important role in lubrication, cell differentiation, angiogenesis, anti-inflammatory response and cell growth. Since HA plays a major role in all wound healing steps, its exogenous application presents the potential to get a faster healing. The presence of the functional groups such as alcohols and carboxylic acids along the backbone of HA allows the introduction of functional domains on it.[20, 21] The addition of functional groups provides the possibility to adjust physical parameters of the films formed with the HA and consequently the cell response to these films can be also influenced. HA is one of the biodegradable polysaccharides that has been broadly studied as a protein carrier. To date, owing to its potential as a drug delivery platform HA has been used as carrier for anti-tumoral and anti-inflammatory drugs.[22-25] Focusing on protein delivery, Mero and colleagues developed a HA-aldehyde derivative as an appropriate platform for the N-terminal site selective conjugation. To achieve that, short pendant chains of 4-aminobutyraldehyde were introduced on the HA backbone.[26] The main advantage of the aldehyde moieties attached on the polymeric chain is that under physiological conditions they can react with a wide range of amino compounds. Another possible type of oxidized HA is the HA derivative with aldehyde groups in position 6 of the N-acetyl-D-glucosamine part.[27, 28] Unlike materials prepared by standard oxidation of HA with sodium hypochlorite, this polymer consists of intact saccharide rings plausibly mimicking the structure of the native HA backbone.[26] Its capability to react with lysine was also successfully proved[29] which indicates that this polymer is promising for the interaction with polylysine in a multilayer system. Thus, the polyelectrolyte multilayer films formed by self crosslinking of PLL and HA-Aldehyde without

any addition of elements or stimuli, will constitute an advantage compared to PEMs crosslinked with the chemicals like EDC/NHS for example. HA-aldehyde and PLL can interact *i)* via formation of ionic pairs where the cations are the protonated amino groups of PLL and the anions are the carboxylic groups of HA, and *ii)* via formation of a covalent imine bond –CH=N- between aldehyde moities of HA and amine groups of polylysine. HA-aldehyde and PLL interactions (ionic and covalent) are summarized in Scheme 1.
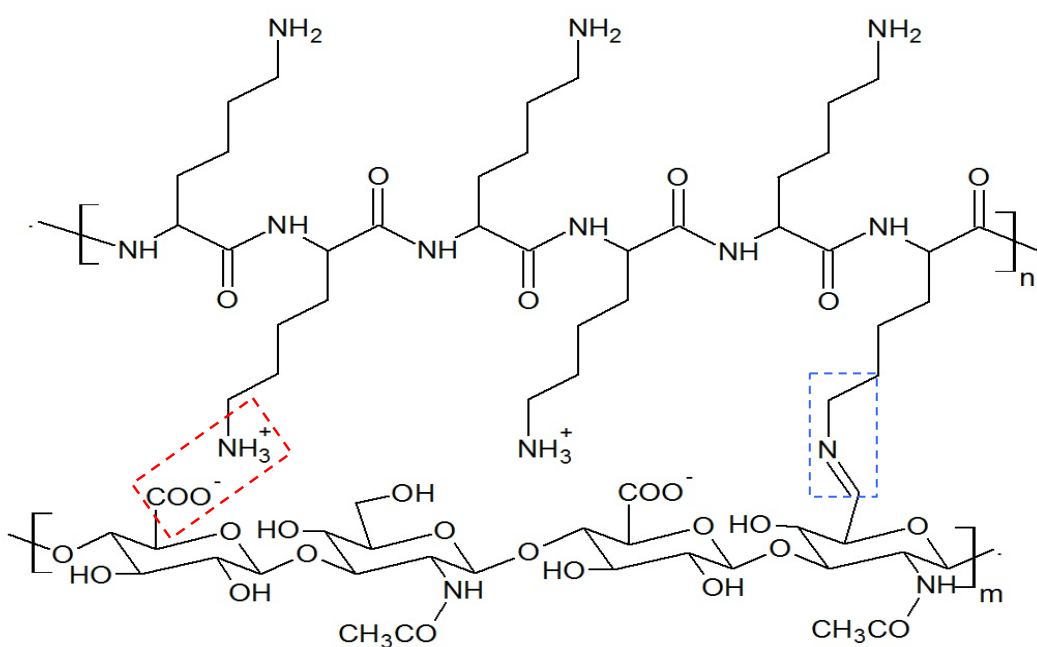

Scheme 1. Covalent and ionic interactions of PLL and HA-aldehyde chains in a layer-by-layer deposited film. The upper chain corresponds to PLL and the lower chain corresponds to HA-aldehyde. An ionic bond between NH_3^+ moiety from PLL and COO^- moiety from HA^- is shown (red rectangle) and a covalent imine bond resulting from the spontaneous reaction of the aldehyde group of HA with an amine group of PLL is drawn (blue rectangle).

Frequently, adverse immune reactions against the implanted materials take place in the host body, which could compromise an orderly tissue repair. Indirect inflammatory responses can be induced by implants in the long term, leading to detrimental effects and damage to the surrounding tissues.[30] One of the key components of inflammation and subsequent events are macrophages. They are cells with considerable phenotypic plasticity which are generally described within two extreme conditions. The pro-inflammatory M1 macrophage is associated with classic signs of inflammation whereas, the pro-healing M2 macrophage stimulates tissue repair, immunoregulation and tissue remodeling.[31] In wound healing process, at early stages a pro-inflammatory M1 phenotype is dominant, whereas in later stages this is shifted towards a pro-healing M2 phenotype. It is known that M1 phenotype macrophages initiate angiogenesis, whereas M2 macrophages stabilizes the growing vasculature. The success or failure of a material device is strongly dependent on the inflammatory response.[31-33] Thus, surface coatings which can provide long term release of M2 inducing cytokines would help in the resolution of inflammation around the implanted materials and can contribute to the faster healing and implant integration (more details can be found in the Supporting Information).

The Layer-by-Layer technique is a well-known method to obtain bioactive coatings with multiple functionalities.[34] The obtained multilayers are widely used as controlled-release drug systems without changing their biological function within the coating.[35-38] Sukhishvili *et al.* have recently reported a coating with a "self-defense" behavior that promotes the release of different dose of antibiotic in function of the decrease of the pH around the surface due to the presence of bacteria.[39] Here, we report, for the first time, polyelectrolyte multilayers films made of poly-(L-lysine) and hyaluroanan-aldehyde (PLL/HA-Ald) derivative, which possess the main advantage to form stable structures through an auto-crosslinking mechanism. Their physicochemical

properties could enable the release of M2-promoting cytokines such as interleukin-4 (IL-4), to promote differentiation of incomming macrophages in the M2 phenotype (anti-inflammatory and remodeling promotion) (Scheme 2).
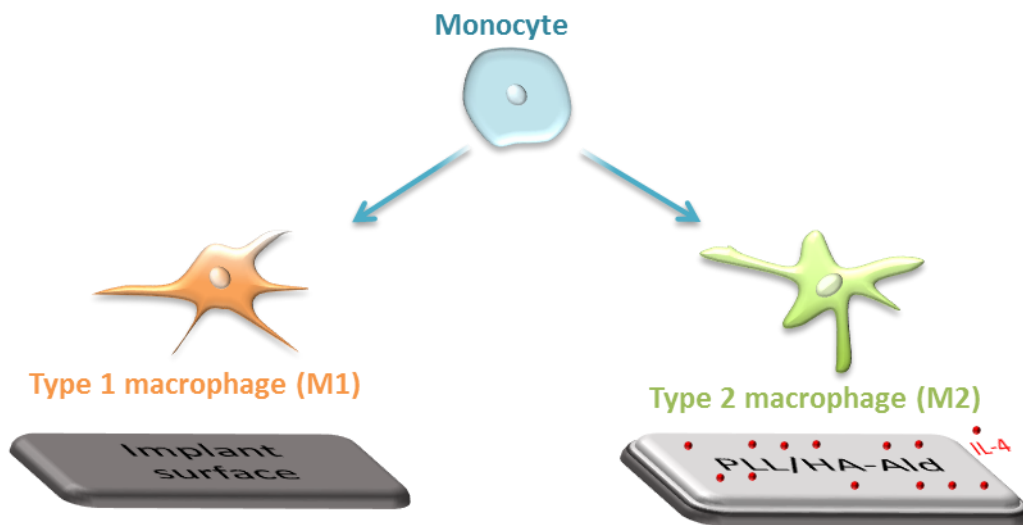

Scheme 2. Macrophage differentiation into M2 type is promoted by the implant surface and presence of IL-4 release system.

1. Experimental Section

Synthesis of HA-aldehyde.

For the preparation of 1 g of HA-aldehyde (sodium formyl hyaluronate or sodium 6(GlcNAc)-oxo hyaluronate) 1.1 g of sodium hyaluronate (436 kDa, ContiPro) is dissolved in 100 mL of demineralized water containing 5 equivalents of disodium hydrogen phosphate (Lach-Ner Ltd, Czech Republic). It was added 0.01 equivalent of the catalyst (TEMPO) and the mixture was

stirred. The following step was the addition of 0.5 equivalent of sodium hypochlorite at 5°C (Scheme 3). The reaction solution was then stirred for 2h at this temperature. The final product was isolated by dialysis (cut off 12 kDa) against demineralized water and by freeze-drying procedure.

HA-aldehyde

HA-aldehyde (hydrated form)
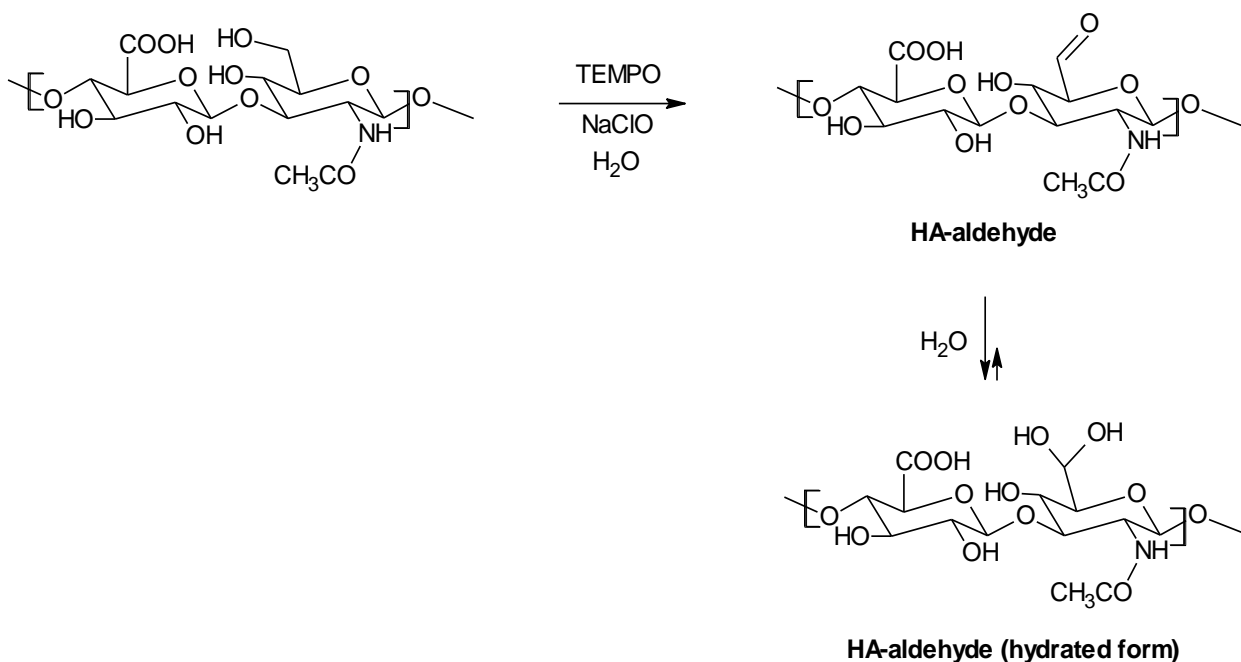
Scheme 3. Synthesis of HA-Aldehyde derivative verified by ^{1}H NMR (D$_2$O) (Supporting Information Figure S1).

Production of PLL/HA multilayers

(PLL, M$_w$ = 52 k Da) was obtained from Alamanda Polymers (Huntsville, USA). Hyaluronic acid (HA, 300 kDa) and HA-Aldehyde (HA-Ald, 436 kDa) were produced and characterized as

described in the literature.[27-29] HA-aldehyde derivative is crosslinked to PLL through hydrolytically labile imine bonds between amino groups of PLL and aldehydic derivative of HA.

Polyelectrolyte solutions were prepared in 0.15 M NaCl/10mM Tris buffer at a concentration of 0.5 mg.mL^{-1}. Multilayer film build up was prepared with a dipping robot (Riegler & Kirstein GmbH, Berlin, Germany) on glass slides (12 mm in diameter). The first layer was Poly(L-lysine) and after each dipping step of 8 minutes the film was washed in rinsing buffer for 5 min (0.15 M NaCl/10mM Tris buffer). The polyanions hyaluronic acids (HA or HA-Ald) were deposited in the same way. The build-up process was continued until 24 bilayers of PLL and HA (or HA-Ald) were formed.

Monitoring of the build-up process by quartz crystal microbalance (QCM)

The build-up process of the multilayer were examined *in situ* by a QCM (Q-Sense 401 flow module QCM-D E1, Q-Sense, Västra Frölunda, Sweden). The molecule adsorption induces the quartz crystal, changing the resonance frequency *f* of it. The quartz crystal was excited at its fundamental frequency of 5 MHz and its third harmonic frequency (denoted by $v = 3$) at 15 MHz was monitored. During each step of molecule adsorption the changes in the resonance frequency, (Δf) were obtained. The crystal used for these experiments is coated with a SiO_2 film (100 nm thick - QSX 303 crystal from Q-Sense). In first approximation, the diminution of the normalized frequency shift, $-\Delta f/v$, is be related with a growth of the adsorbed mass on the crystal.[40]

Determination of film thickness

The thickness of the films were obtained by confocal laser analysis. For that, it was used a Zeiss confocal microscope (LSM, 710) using a 40x (Zeiss Achroplan) objective. Polyelectrolyte

films were labeled by deposition of a FITC (fluorescein-5-isothiocynanate) labelled PLL (PLL-FITC, Mw = 3.89×10^2 Da, Sigma Aldrich, France) on top of the film. After excitation, FITC fluorescence was detected by argon laser with a cut-off dichroic mirror of 488 nm and emission band-pass filter 493-556 nm (green emission). Virtual vertical sections (x,z) can be obtained, therefore allowing approximate thickness of the film.[41]

Determination of molecular mobility by FRAP (Fluorescence Recovery After Photobleaching) experiments

The mobility of PLL-FITC and polyelectrolyte chains within the films was qualitatively determined by the FRAP experiments. Briefly, a circular area of 50 μm^2 of the image (256x256 pixels) was bleached with the laser set at its maximum power. Then, the disappearance of the bleached area and the eventual recovery of the fluorescence were observed at various time periods. The rate of recovery of fluorescence in the bleached area is an indirect measurement of the mobility of the fluorescence molecule, *i.e.* PLL-FITC chains.[10]

Release kinetics of Bovine Serum Albumin (BSA) from the films

Release experiments of fluorescently labelled BSA (BSA-FITC) were carried out with a SAFAS Genius XC spectrofluorimeter (Monaco). PLL/HA films were incubated with BSA-FITC solution (1 mg.mL^{-1}) for 1 hour and then rinsed 3 times with PBS during 5 minutes. The release experiments were performed in PBS solution and the data were monitored every 5 minutes during 24 hours. The measurement parameters were $\lambda_{ex}/\lambda_{em}$ = 495nm/520nm.

Before monitoring the release, the quantification of BSA-FITC loaded on the films was done by confocal analysis. The method consisted in using a calibration curve by plotting the

fluorescence intensities of BSA-FITC solutions (image sections) as a function of their known concentrations. Then, fluorescence intensities of the image sections of the loaded film were measured and thanks to the calibration curve the concentration of BSA-FITC was determined.[42]

Release kinetics of IL-4 from the films

The levels of cytokines were measured with ELISA Development Kits. Standard curves were constructed with the included standard protein in phosphate buffer. Samples were analysed according to the manufacturer's protocol. Absorbance was measured at 450 nm with SpectraMax Paradigm. Cytokine concentrations were calculated from the best fit line constructed from the standard sample dilutions' OD values plotted against their concentrations. Cytokine concentrations were calculated from two parallels of one sample. OD cutoff represents the background OD value which corresponds to a standard concentration of 0 ng/mL on the best fit line. Minimal detection limit corresponds to the minimal cytokine concentration that can be detected with the used ELISA Development Kit according to the manufacturer.

AFM nanoindentation for elastic modulus analysis

AFM experiments were done with a MFP3D-BIO instrument (Asylum Research Technology, Atomic Force F & E GmbH, Mannheim, Germany). The Young's modulus is calculated by the nanoindentation method. The spring constants of the cantilevers measured, using a thermal noise method, were found to be 60 pN/nm. Triangular cantilevers with colloidal probe (borosilicate glass sphere with a radius of 10 μm, with approach speed of 10 μm/s) were purchased from Novascan (Novascan Technologies, Inc. Iowa State University Research Park, IA 50010 USA). The experiments were done at room temperature in saline buffer solution at pH 7.4. A grid map of 32-by-32 force curves was recorded at different locations of the film surface for obtaining the

mechanical properties. 15 nN were the maximal loading force. Elasticity maps were calculated based on Dimitriadis model: [43]

$$F = \frac{4E}{3(1-\nu^2)} R^{1/2}\, \delta^{3/2} \left[1 + 1{,}133\chi + 1{,}283\chi^2 + 0{,}769\chi^3 - 0{,}0975\chi^4\right] \qquad [1]$$

where δ is the indentation depth, ν the Poisson coefficient, R is the colloids radius and h the sample thickness. The Dimitriadis correction for finite thickness is defined by χ parameter:

$$\chi = \frac{\sqrt{R\delta}}{h} \qquad [2]$$

All the curves were analyzed by mean of an automatic Matlab algorithm described elsewhere.[44]

Contrary to the classical Hertz model, Dimitradis model was used in order to take into account the mechanical contribution of both the finite thickness of the soft polyelectrolyte film and the influence of the supporting hard substrate (glass). Furthermore, Dimitriadis model described the mechanical behavior of a finite elastic sample under sphere/plane contact. Such geometrical configuration is more relevant than the Hertzian description of paraboloid/plane contact.[43]

Primary monocyte culture on PLL coating films

Buffy coats were obtained from the National Blood Service (U.K.) following Ethics committee approval. Peripheral blood mononuclear cells (PBMCs) were obtained from heparinised blood by Histopaque-1077 (Sigma-Aldrich) density gradient centrifugation. Monocytes were isolated from PBMCs using the MACS magnetic cell separation system (positive selection with CD14 MicroBeads and LS columns, Miltenyi Biotec) as we have previously described.[45] This method

routinely yielded 95% pure monocytes as determined by flow cytometric analysis of CD14 expression.

Purified monocytes were cultured at 1 x 10^6 cells / mL / well in RPMI-1640 supplemented with 10% fetal bovine serum (FBS), 2 mM L-glutamine, 100 U.mL^{-1} penicillin, and 100 µg.mL^{-1} streptomycin (all from Sigma-Aldrich) in 12-well tissue culture-treated plates containing the coated films. Samples and controls were incubated at 37°C, 5% CO_2 for 1, 3 and 6 days. Scheme 4 shows the time line of the experiments and the readouts made.
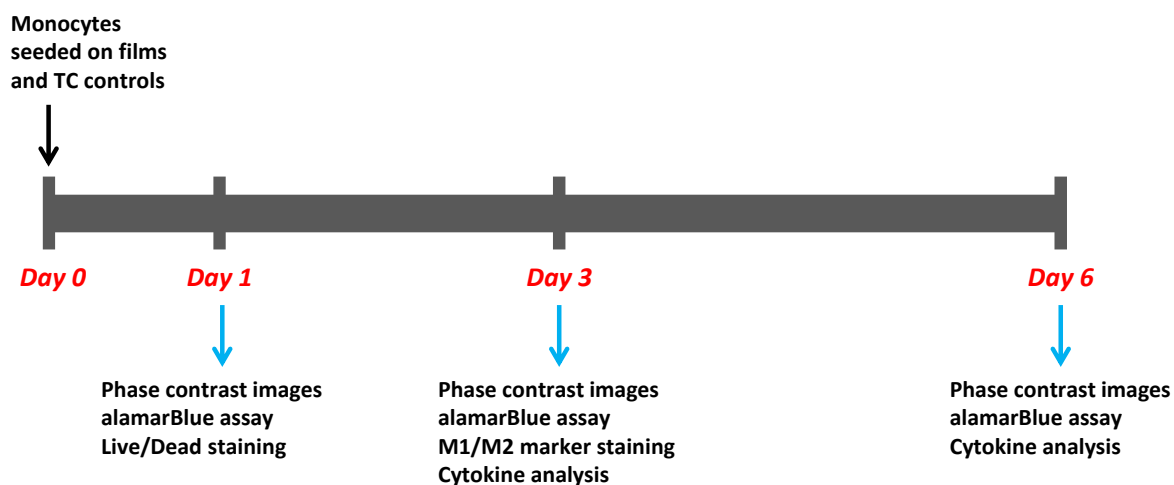
Scheme 4. Time line of human primary monocyte culture on PLL/HA-Ald films and controls.

Phase contrast microscopy

Phase contrast images were captured using an Olympus CDX41 microscope (Olympus Corporation, Japan) with an Infinity 2 camera and Infinity Analyze software.

Blue assay

The AlamarBlue assay kit (Thermo Fisher Scientific, USA) was used to determine the cell viability as per the manufacturer's instructions. Controls were monocytes plated in 12-well tissue culture-treated plates in the same medium in the absence of any cytokines (TC control).

Cytokine analysis

Supernatants were collected and assayed for the cytokines TNF-α, IL-12, IL-1β, CCL18 and IL-1RA by ELISA as per the manufacturer's instructions (Table 1).

Table 1. ELISA kits and standard/sample dilutions

Cytokine	ELISA Kit supplier
IL-4	PeproTech 900-K14
IL-1β	Antibody Solutions AS56-P, AS57-B (Capture and detection antibodies) Peprotech 200-01B (Standard protein)
IL-1RA	PeproTech 900-K474
IL-12	PeproTech 900-K96
CCL18	R&D Systems DY394
TNFα	Peprotech 900-K25

2. Results and Discussion

2.1. *PLL/HA and PLL/HA-Aldehyde polyelectrolyte multilayer film characterizations*

The build-up process of the multilayered films was monitored *in situ* by quartz crystal microbalance-dissipation. In first approximation, decreases in the normalized resonance frequency $-\Delta f/\nu$ can be associated with a variation of the mass adsorbed on the crystal. The

evolution of $-\Delta f/v$ with the number of deposited layers are exponential for both PLL/HA and PLL/HA-Ald, (Figure 1). However in the case of covalent multilayers, the mass adsorbed for a given number of layers appears slightly higher than for non-covalent multilayers. Many parameters could be at the origin of the difference in these growth like molecular weight of HA (300 kDa for HA and 436 kDa for HA-Ald) or the covalent binding of HA-Ald to PLL.
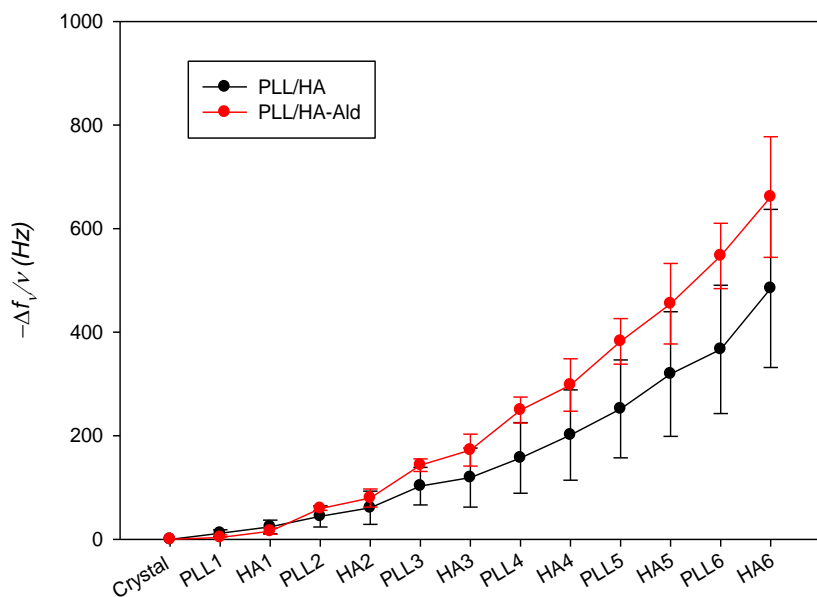

Figure 1. Buildup at pH 7.4 /150 mM NaCl of $(PLL/HA)_6$ and $(PLL/HA-Ald)_6$ multilayer films on a SiO_2-coated crystal followed by QCM-D, evolution of normalized frequency $-\Delta f/v$

Section images of $(PLL/HA)_{24}/PLL\text{-}FITC/HA$ and $(PLL/HA\text{-}Ald)_{24}/PLL\text{-}FITC/HA\text{-}Ald$ multilayer deposited on glass slides are presented in Figure 2. Confocal section images depict for both films a homogeneous of PLL-FITC distribution throughout more than 4 μm which probably corresponds to the entire film thickness as it was stated previously for non-crosslinked films.[46] This may be attributed to the diffusion of mobile PLL-FITC chains in and out of the film due to

interlayer mixing of HA and PLL-FITC. This also suggests that despite formation of covalent bonding due to the presence of HA-Ald in (PLL/HA-Ald)$_{24}$ multilayers, some PLL-FITC chains are able to diffuse at least during the build up process.
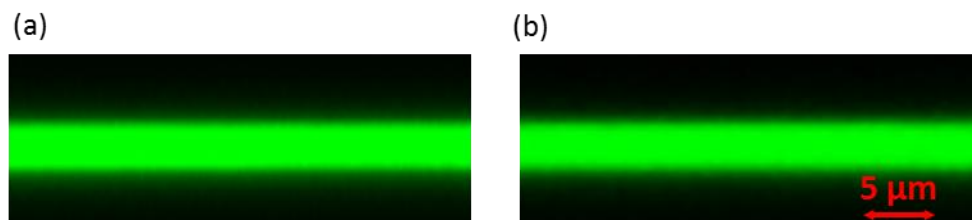

Figure 2. Section images, obtained by confocal laser scanning microscope, of multilayer films deposited on glass slides: (a) (PLL/HA)$_{24}$/PLL-FITC/HA and (b) (PLL/HA-Ald)$_{24}$/PLL-FITC/HA-Ald.

Nanoindentation measurements were then performed with AFM to determine the mechanical properties of both films. It is observed that PLL/HA-Ald film is more rigid than PLL/HA, with statistically significant difference in Young Moduli of 142 ± 63 kPa for PLL/HA-Ald and 10 ± 4 kPa for PLL/HA ($P<0.001$). This strongly indicates the crosslink of HA-Aldehyde chains through the reaction of hydrolytically labile imine bond between aldehydic derivative of HA and amino groups of PLL chains (Scheme 1). Increase in the Young modulus could be advantageous for biological applications where hard substrates are generally better for cell proliferation.

Then, FRAP experiments (fluorescence recovery after photobleaching) were performed and showed that after bleaching a circular area in the PLL/HA film, the green fluorescence corresponding to PLL-FITC chains was almost (80%) totally recovered after 50 minutes (Figure 3). This found recovery was due to lateral mobility of the PLL chains within the film. It was previously demonstrated that about 70% of PLL chains are mobile in a non-cross-linked

PLL/HA film.[47] In comparison, when PLL/HA-Ald was used, the recovery of fluorescence was slower. This indicates that mobility of PLL-FITC in PLL/HA-Ald is lower than that on PLL/HA, and it could suggest that some PLL-FITC chains are crosslinked and could not diffuse any more. From Figure 3, we can conclude that almost 40% of the fluorescence is recovered in PLL/HA-Ald and thus about 60% of PLL chains are immobile. Finally FRAP experiments confirm that HA-Ald is able to crosslink the film. In comparison with the more conventional method using EDC, HA-Ald is a self-crosslinking method that do not need any additional steps with chemicals after the film buildup.

PLL/HA films are known to have the capacity to be loaded with a high amount of proteins like Human Serum Albumin [42] or drugs like paclitaxel.[48] However little is known on this aspect for covalent multilayers and nothing is known for HA-Ald. In order to study the release behavior of our multilayer films, the FITC-labeled bovine serum albumin (BSA-FITC) and interleukin 4 (IL-4) were loaded on the top of the films. BSA is used as a model protein and IL-4 is the cytokine selected for our immunomodulation studies described later. BSA-FITC (100 µL) was deposited for 1h at a concentration of 1 mg.mL^{-1} on top of either PLL/HA or PLL/HA-Ald films. After rinsing steps, it was observed by confocal analysis that there is no difference in amounts of BSA-FITC adsorbed on PLL/HA or on PLL/HA-Ald films, in each case the concentration of BSA in the film was 35 mg.mL^{-1} of BSA-FITC (see Supplementary Information Figure S2 for calibration curve), which corresponds to 14 µg of BSA loaded per cm^2 on each film. This suggests that both film can be loaded with a high amount of BSA greater than the solution concentration (1mg.mL^{-1}) and finally they act as a kind of "sponge" for proteins. This renders such coatings of high interest to functionalize biomedical devices.

Release kinetics of BSA out of multilayer films in presence of PBS was investigated by fluorimetry. The release profiles seem to be dependent on the film crosslinking, the release of BSA-FITC from PLL/HA-Ald is slower for the first 24 hours than for non-crosslinked PLL/HA films (Figure 4a). This constitutes an interesting property as effectiveness of the PLL/HA film to release a protein can probably be tuned by playing with the crosslinking degree (HA/HA-Ald ratio for example) and moreover long-term release can probably be reached with PLL/HA-Ald films. The BSA-FITC release kinetics was also monitored in presence of medium containing serum, to mimic the concentration of proteins present in blood/interstitial fluid *in vivo* (Supplementary Information Figure S3). For non-crosslinked PLL/HA films, the release of BSA-FITC is almost similar when PBS or media containing serum have been used as supernantant : 0.08 mg.mL^{-1} is released after 24h in both cases. However for crosslinked PLL/HA-Ald films the amount of BSA-FITC released after 24h is about 3 times higher in complete medium compared to PBS. Finally the slower release and thus the higher affinity of BSA to PLL/HA-Ald films can be attributed to higher hydrophobicity in these films because covalent PLL/HA interaction could be more tight and could release more water.

Then we focused our study on the release of interleukin 4 (IL-4), a key cytokine in type 2 immunity, which is also essential for anti-helminth protection, wound healing, and allergy.[49] This protein with a molecular weight of 15 kDa is positively charged at pH 7.4 (pI=9.17). From QCM experiments, we monitored a loading rate of IL-4 corresponding to an increase of normalized frequency value of about 75 Hz for (PLL/HA)$_6$ and (PLL/HA-Ald)$_6$ films (data not shown), which means that the same adsorbed amount of the cytokines was adsorbed for both films. Unlike BSA, IL-4 released at the first 48 hours is significantly higher for PLL/HA-Ald films compared to PLL/HA films (t-test, P ≤0.042, n=3), (Figure 4b). Finally this means that PLL/HA-

Ald films have better mechanical property than PLL/HA films due to the crosslinking however they maintain the same ability to release IL-4.
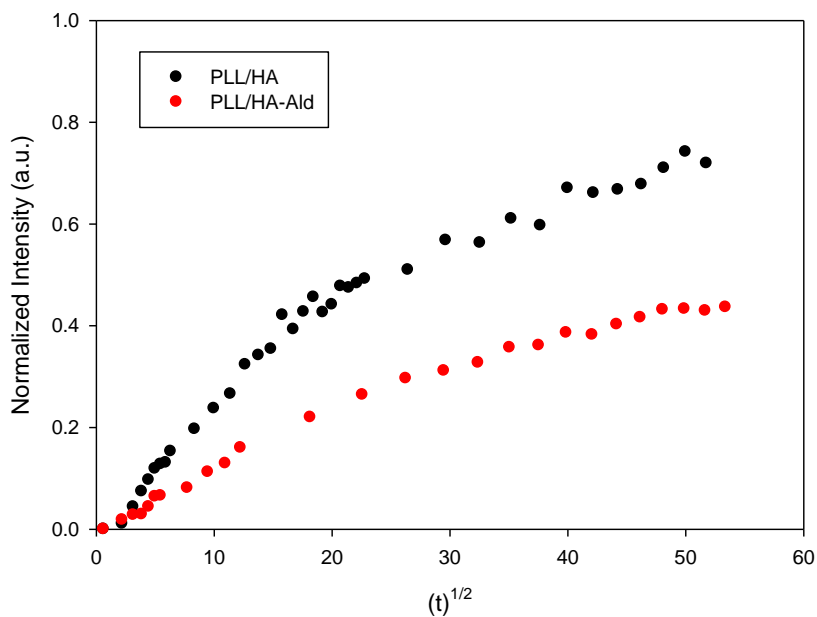

Figure 3. Fluorescence recovery in a (PLL/HA)$_{24}$-PLL-FITC-HA (HA) and in a (PLL/HA-Ald)$_{24}$-PLL-FITC-HA-Ald (Ald) after photobleaching as a function of time after bleaching.
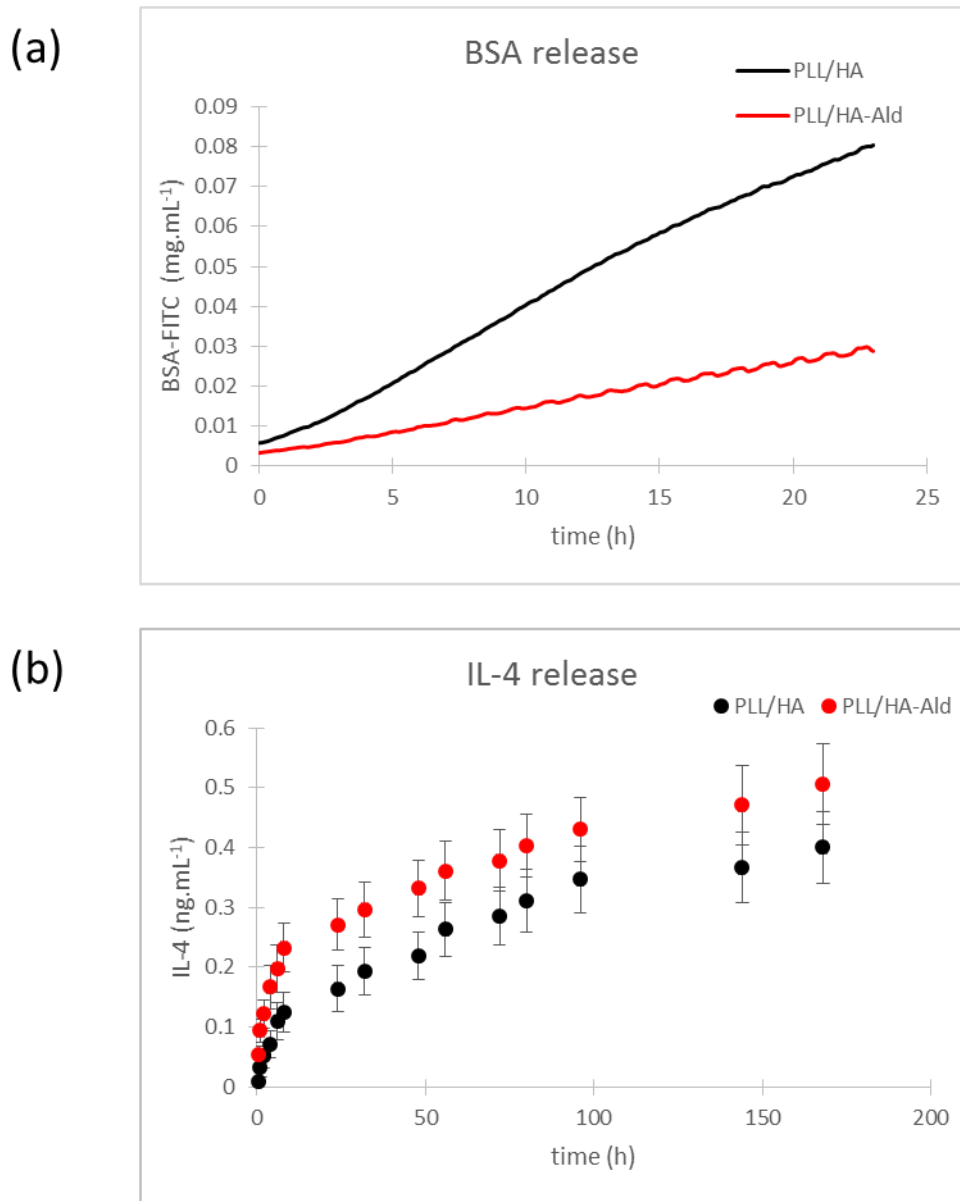
Figure 4. Kinetic of biomolecules release from PLL/HA and PLL/HA-Ald in presence of PBS: (a) BSA-FTIC and (b) IL-4.

3.2 Monocyte phenotype and behavior on PLL/HA and PLL/HA-Ald multilayers

In order to determine, whether the release of IL-4 can control macrophage phenotype on PLL/HA films, primary monocytes were seeded on the films in the presence and absence of IL-4.

On day 3 monocytes seeded on PLL/HA and PLL/HA-Ald films with or without IL-4, appeared similar in size and morphology (Figure 5a). On day 6 monocytes on PLL/HA in presence or absence of IL-4 remained small and spherical, whereas monocytes on PLL/HA-Ald appeared larger and some adherent cells were observed on the PLL/HA-Ald films, in particular on IL-4 loaded films (Figure 5b).
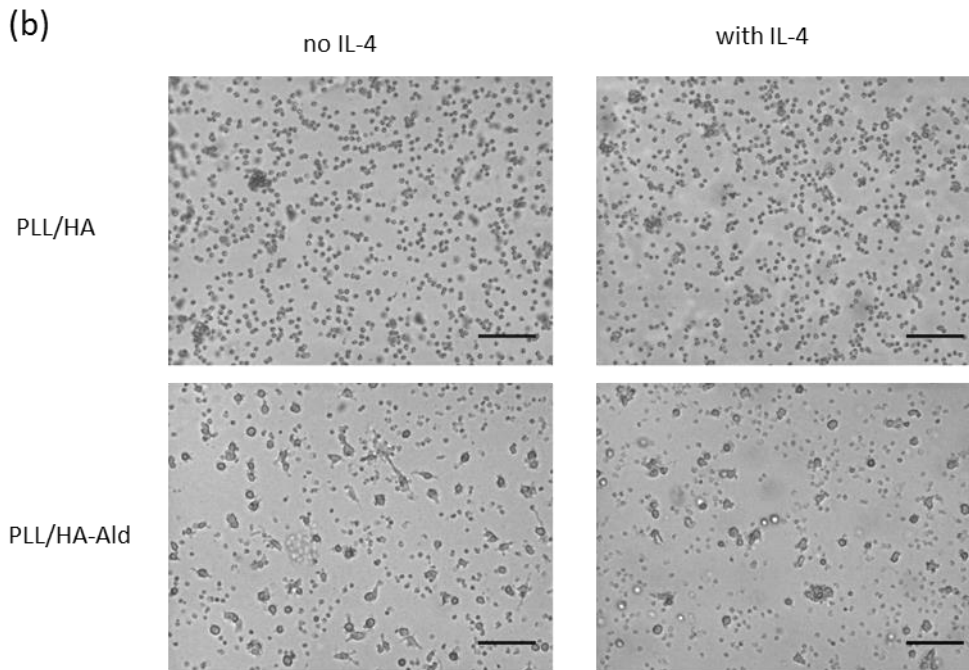
(b)

no IL-4 with IL-4
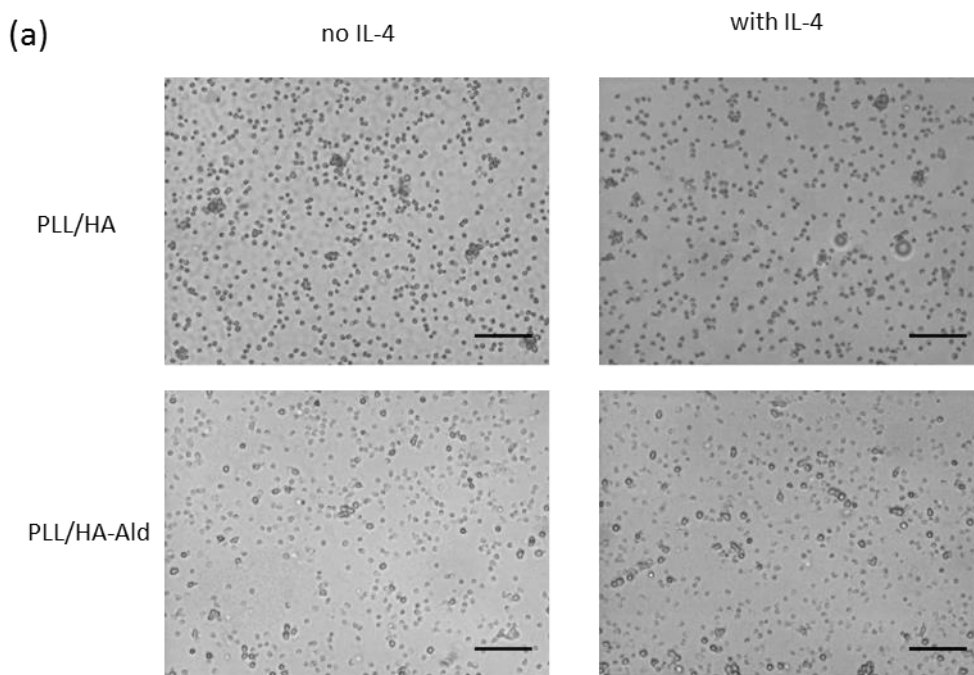
PLL/HA

PLL/HA-Ald

Figure 5. Phase contrast images of monocytes seeded on the films after (a) 3 and (b) 6 days of culture on PLL/HA and PLL/HA-Aldehyde in presence or not of IL-4. Scale bar = 100 μm.

The metabolic activity of the cells was evaluated and it was shown to be time-dependent for all conditions (Figure 6). On day 1 and 6, there was no apparent difference in viability among PLL/HA and PLL/HA-Ald groups with or without IL-4. Cells seeded on PLL/HA-Ald show the highest viability on day 3, with the highest value compare to PLL/HA and PLL/HA-Ald groups (Figure 6).
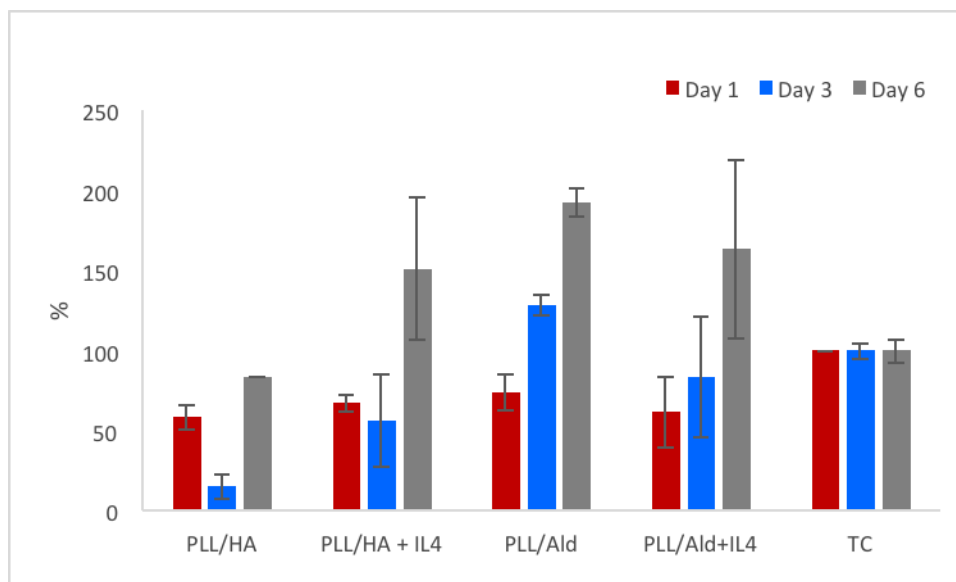
Figure 6. Metabolic activity of monocytes seeded on PLL/HA and PLL/HA-Ald with or without IL-4 after 1, 3 and 6 days (AlamarBlue assay). Controls were monocytes plated in well tissue culture-treated plates in the same medium in the absence of any cytokines (TC control, 100%).

The cells seeded on PLL/HA without IL-4 produced high levels of pro-inflammatory cytokines (TNF-α, IL-12, and IL-β). This shows that the monocytes are easily activated to pro-inflammatory macrophages due to the surface. However, the level of pro-inflammatory cytokines TNF-α was strongly reduced at day 3 and day 6 on PLL/HA-Ald films even in absence of IL-4 (Figure 7 a, b). Moreover, addition of IL-4 on PLL/HA films also strongly reduced TNF-α production compare to non-functionalized PLL/HA. Production of IL-12, a second proinflammatory cytokine, was quite high at day 3 on PLL/HA or PLL/HA-Ald. However adding IL-4 reduced the production (Figure 7c). At day 6, a similar effect was observed for PLL/HA films (Figure 7d). Also, IL-4 functionalized films strongly reduced the level of the proinflammatory IL-1β at day 3 or day 6 (Figure 7 e, f). Finally, these results suggest that the crosslinking of PLL/HA films inhibit the differentiation of macrophage phenotype into a pro-

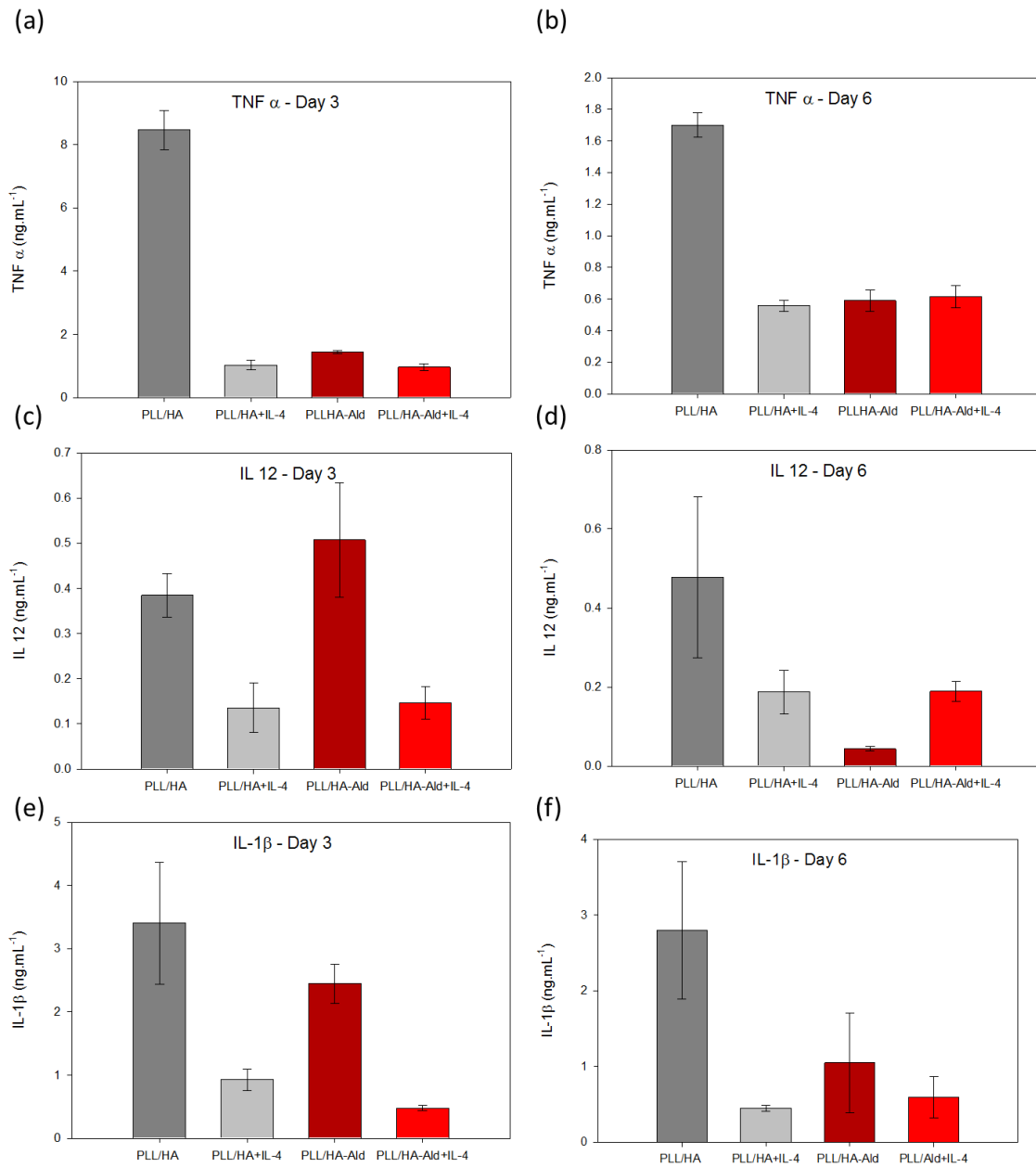inflammatory (M1 type). Moreover, adding IL-4 in the films also limit the pro-inflammatory macrophages.

(a)

(b)

(c)

(d)

(e)

(f)

Figure 7. Pro-inflammatory cytokines produced from monocytes seeded on PLL/HA, PLL/HA-Ald with or without IL-4: TNF-α after 3 (a) and 6 days (b); IL-12 after 3 (c) and 6 days (d), IL-1β after 3 (e) and 6 days (f).

Regarding anti-inflammatory cytokine production, monocytes seeded on PLL/HA and PLL/HA-Ald produced IL-1RA. However, the presence of IL-4 increased the amount at day 3 for PLL/HA and PLL/HA-Ald and at day 6 for PLL/HA (Figure 8a, b). In the case of PLL/HA-Ald, IL-1RA production on day 6 was similar in the presence or absence of IL-4 (Figure 8b). On the contrary, CCL18 production by cells on PLL/HA films occurred only in presence of IL-4 (Figure 8c, d). Once again, cells on PLL/HA-Ald films produced CCL18 in the absence of IL-4 (on day 3 or 6), but production was higher when the films had been loaded with IL-4, (Figure 8c, d). These results with anti-inflammatory cytokines mainly confirm those obtain with the pro-inflammatory, *i.e.* both crosslinking of the film and addition of cytokines IL-4 drive the differentiation into M2 macrophages over M1 macrophages.
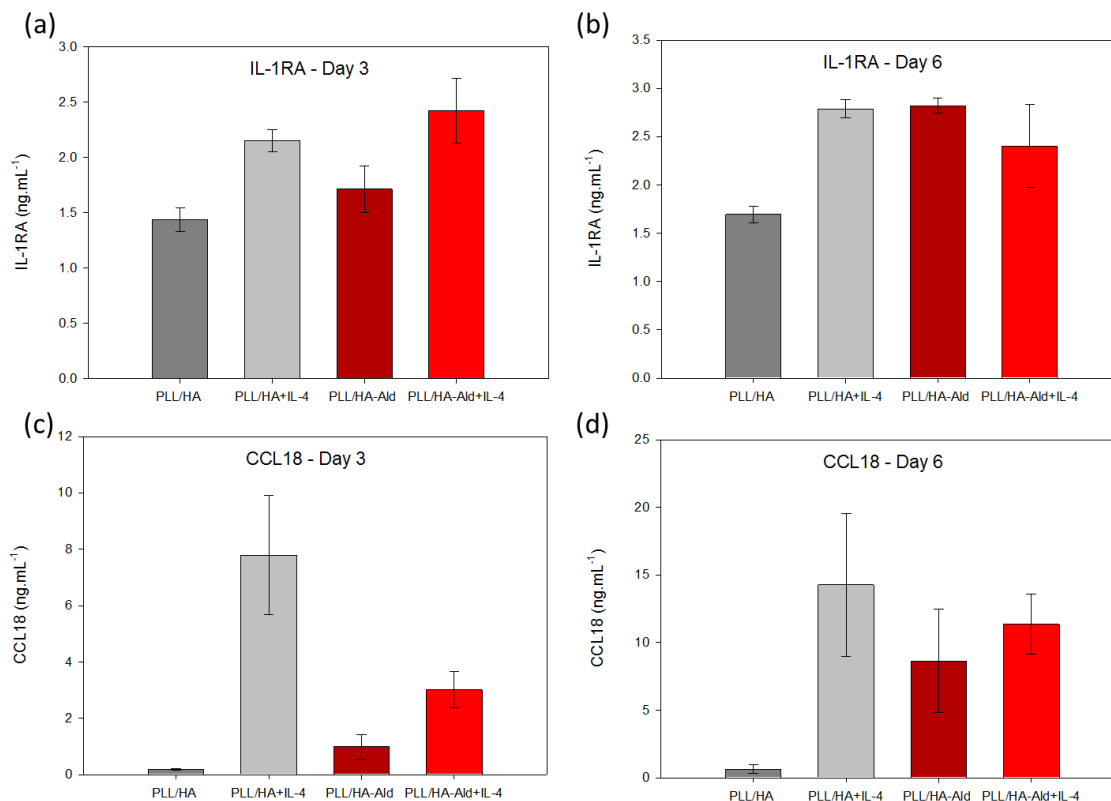
Figure 8. Anti-inflammatory cytokines produced from monocytes seeded on PLL/HA, PLL/HA-Ald with or without IL-4: IL-1RA after 3 (a) and 6 days (b), CCL18 after 3 (c) and 6 days (d).

Finally, PLL/HA-Ald films could have applications where anti-inflammatory / pro-wound healing macrophage populations would be beneficial in improving the rate and quality of implant integration, protection of biomedical devices such as electrodes from adverse immune reactions.

Conclusions

In summary, the results show that polyelectrolyte multilayers made of PLL and HA-aldehyde derivative can be successfully built. The introduction of the bioactive molecules, interleukin-4, can be used for functionalization these films. Moreover, drug release behavior could be

modulated by tuning the physical property of the films, such as Young Modulus. The main objective of this study is to use the controlled release capacities of the PLL/HA films for the delivery of immunomodulatory cytokines such as IL-4. PLL/HA-Aldehyde films stimulate the anti-inflammatory response on monocytes even in the absence of IL-4. However IL-4 improves in an efficient way the anti-inflammatory properties of the coating. The designed film could be applied in the future to medical devices like implants to trigger differentiation of monocytes in a pro-healing phenotype. Such coatings can be used in the control of initial inflammatory reactions to permanent titanium implants such as dental, orthopaedic replacement systems or in neuroprosthetic devices in the brain. We plan to use these coatings also for improvement of integration of recently developed artificial larynx system that is clinical trial stage.

Supporting Information

Additional information regarding the Interleukin 4, inflammatory responses, characterization of HA-Aldehyde by ^{1}H NMR and calibration curve for BSA-FITC are found in Supporting Information.

Author Contributions

The manuscript was written through contributions of all authors. All authors have given approval to the final version of the manuscript.

Funding Sources

REFERENCES

(1) Lavalle, P.; Voegel, J. C.; Vautier, D.; Senger, B.; Schaaf, P.; Ball, V., Dynamic aspects of films prepared by a sequential deposition of species: perspectives for smart and responsive materials. *Adv. Mater.* **2011,** *23*, 1191-1221.

(2) Lvov, Y.; Decher, G.; Moehwald, H., Assembly, structural characterization, and thermal behavior of layer-by-layer deposited ultrathin films of poly(vinyl sulfate) and poly(allylamine). *Langmuir* **1993,** *9*, 481-486.

(3) Tieke, B.; Van Ackern, F.; Krasemann, L.; Toutianoush, A., Ultrathin self-assembled polyelectrolyte multilayer membranes. *Europ. Phys. J. E.* **2001,** *5*, 29-39.

(4) Pargaonkar, N.; Lvov, Y. M.; Li, N.; Steenekamp, J. H.; de Villiers, M. M., Controlled release of dexamethasone from microcapsules produced by polyelectrolyte layer-by-layer nanoassembly. *Pharmaceut. Res.* **2005,** *22*, 826-835.

(5) Prokopović, V. Z.; Duschl, C.; Volodkin, D., Hyaluronic Acid/Poly-l-Lysine Multilayers as Reservoirs for Storage and Release of Small Charged Molecules. *Macromol. Biosci.* **2015,** *15*, 1357-1363.

(6) Volodkin, D.; von Klitzing, R., Competing mechanisms in polyelectrolyte multilayer formation and swelling: Polycation–polyanion pairing vs. polyelectrolyte–ion pairing. *Curr. Opin. Colloid Interface Sci.* **2014,** *19*, 25-31.

(7) Brunot, C.; Grosgogeat, B.; Picart, C.; Lagneau, C.; Jaffrezic-Renault, N.; Ponsonnet, L., Response of fibroblast activity and polyelectrolyte multilayer films coating titanium. *Dent. Mater.* **2008,** *24*, 1025-1035.

(8) Almodóvar, J.; Guillot, R.; Monge, C.; Vollaire, J.; Selimović, Š.; Coll, J.-L.; Khademhosseini, A.; Picart, C., Spatial patterning of BMP-2 and BMP-7 on biopolymeric films and the guidance of muscle cell fate. *Biomaterials* **2014,** *35*, 3975-3985.

(9) Müller, S.; Koenig, G.; Charpiot, A.; Debry, C.; Voegel, J.-C.; Lavalle, P.; Vautier, D., VEGF-Functionalized Polyelectrolyte Multilayers as Proangiogenic Prosthetic Coatings. *Advanced Functional Materials* **2008,** *18*, 1767-1775.

(10) Vrana, N.; Erdemli, O.; Francius, G.; Fahs, A.; Rabineau, M.; Debry, C.; Tezcaner, A.; Keskin, D.; Lavalle, P., Double entrapment of growth factors by nanoparticles loaded into polyelectrolyte multilayer films. *J. Mater. Chem. B* **2014,** *2*, 999-1008.

(11) Gilde, F.; Guillot, R.; Fourel, L.; Almodovar, J.; Crouzier, T.; Boudou, T.; Picart, C., Matrix-Bound Presentation of Bone Morphogenetic Protein 2 by Multilayer Films: Fundamental Studies and Applications to Orthopedics. *Eds C. Picart, F. Caruso and J.-C. Voegel, Wiley-VCH Verlag GmbH & Co. KGaA, Weinheim, Germany* **2015**.

(12) Yamanlar, S.; Sant, S.; Boudou, T.; Picart, C.; Khademhosseini, A., Surface functionalization of hyaluronic acid hydrogels by polyelectrolyte multilayer films. *Biomaterials* **2011,** *32*, 5590-5599.

(13) Hillberg, A. L.; Holmes, C. A.; Tabrizian, M., Effect of genipin cross-linking on the cellular adhesion properties of layer-by-layer assembled polyelectrolyte films. *Biomaterials* **2009,** *30*, 4463-4470.

(14) Picart, C.; Senger, B.; Sengupta, K.; Dubreuil, F.; Fery, A., Measuring mechanical properties of polyelectrolyte multilayer thin films: Novel methods based on AFM and optical techniques. *Colloids Surf. A* **2007,** *303*, 30-36.

(15) Picart, C., Polyelectrolyte multilayer films: from physico-chemical properties to the control of cellular processes. *Curr. Med. Chem.* **2008,** *15*, 685-697.

(16) Ren, K.; Crouzier, T.; Roy, C.; Picart, C., Polyelectrolyte multilayer films of controlled stiffness modulate myoblast cells differentiation. *Adv. Funct. Mater.* **2008,** *18*, 1378.

(17) Schneider, A.; Richert, L.; Francius, G.; Voegel, J.-C.; Picart, C., Elasticity, biodegradability and cell adhesive properties of chitosan/hyaluronan multilayer films. *Biomed. Mater.* **2007,** *2*, S45.

(18) Picart, C.; Elkaim, R.; Richert, L.; Audoin, F.; Arntz, Y.; Da Silva Cardoso, M.; Schaaf, P.; Voegel, J.-C.; Frisch, B., Primary cell adhesion on RGD-functionalized and covalently crosslinked thin polyelectrolyte multilayer films. *Adv. Funct. Mater.* **2005,** *15*, 83-94.

(19) Francius, G.; Hemmerlé, J.; Ohayon, J.; Schaaf, P.; Voegel, J.-C.; Picart, C.; Senger, B., Effect of crosslinking on the elasticity of polyelectrolyte multilayer films measured by colloidal probe AFM. *Microsc. Res. Tech.* **2006,** *69*, 84-92.

(20) Collins, M. N.; Birkinshaw, C., Hyaluronic acid based scaffolds for tissue engineering—A review. *Carbohyd. Polym.* **2013,** *92*, 1262-1279.

(21) Morra, M., Engineering of biomaterials surfaces by hyaluronan. *Biomacromolecules* **2005,** *6*, 1205-1223.

(22) Banzato, A.; Bobisse, S.; Rondina, M.; Renier, D.; Bettella, F.; Esposito, G.; Quintieri, L.; Meléndez-Alafort, L.; Mazzi, U.; Zanovello, P.; Rosato, A., A Paclitaxel-Hyaluronan

Bioconjugate Targeting Ovarian Cancer Affords a Potent In vivo Therapeutic Activity. *Clin. Cancer Res.* **2008,** *14*, 3598-3606.

(23) Homma, A.; Sato, H.; Okamachi, A.; Emura, T.; Ishizawa, T.; Kato, T.; Matsuura, T.; Sato, S.; Tamura, T.; Higuchi, Y., Novel hyaluronic acid–methotrexate conjugates for osteoarthritis treatment. *Bioorg. Med. Chem.* **2009,** *17*, 4647-4656.

(24) Pitarresi, G.; Palumbo, F. S.; Albanese, A.; Fiorica, C.; Picone, P.; Giammona, G., Self-assembled amphiphilic hyaluronic acid graft copolymers for targeted release of antitumoral drug. *J. Drug Target.* **2010,** *18*, 264-276.

(25) Saravanakumar, G.; Choi, K. Y.; Yoon, H. Y.; Kim, K.; Park, J. H.; Kwon, I. C.; Park, K., Hydrotropic hyaluronic acid conjugates: Synthesis, characterization, and implications as a carrier of paclitaxel. *Int. J. Pharm.* **2010,** *394*, 154-161.

(26) Mero, A.; Pasqualin, M.; Campisi, M.; Renier, D.; Pasut, G., Conjugation of hyaluronan to proteins. *Carbohyd. Polym.* **2013,** *92*, 2163-2170.

(27) Buffa, R.; Kettou, S.; Pospisilova, L.; Berkova, M.; Velebny, V. Oxidized derivative of hyaluronic acid, a method of preparation thereof and a method of modification thereof. 2010.

(28) Buffa, R.; Kettou, S.; Pospisilova, L.; Huerta-Angeles, G.; Chladkova, D.; Velebny, V., method of preparation of an oxidized derivative of hyaluronic acid and a method of modification thereof. In Google Patents: 2010.

(29) Šedová, P.; Buffa, R.; Kettou, S.; Huerta-Angeles, G.; Hermannová, M.; Leierová, V.; Šmejkalová, D.; Moravcová, M.; Velebný, V., Preparation of hyaluronan polyaldehyde—a precursor of biopolymer conjugates. *Carbohydrate research* **2013,** *371*, 8-15.

(30) Rostam, H.; Singh, S.; Vrana, N.; Alexander, M.; Ghaemmaghami, A., Impact of surface chemistry and topography on the function of antigen presenting cells. *Biomater. Sci.* **2015,** *3*, 424-441.

(31) Kzhyshkowska, J.; Gudima, A.; Riabov, V.; Dollinger, C.; Lavalle, P.; Vrana, N. E., Macrophage responses to implants: prospects for personalized medicine. *Journal of leukocyte biology* **2015**, jlb. 5VMR0415-166R.

(32) Badylak, S. F.; Gilbert, T. W., Immune response to biologic scaffold materials. *Semin. Immunol.* **2008,** *20*, 109-116.

(33) Ratner, B. D.; Hoffman, A. S.; Schoen, F. J.; Lemons, J. E., *Biomaterials science: an introduction to materials in medicine*. Academic Press: 2004.

(34) Decher, G.; Schlenoff, J. B., *Multilayer thin films: sequential assembly of nanocomposite materials*. John Wiley & Sons: 2006.

(35) Gribova, V.; Auzely-Velty, R.; Picart, C., Polyelectrolyte multilayer assemblies on materials surfaces: from cell adhesion to tissue engineering. *Chem. Mater.* **2011,** *24*, 854-869.

(36) Tang, Z.; Wang, Y.; Podsiadlo, P.; Kotov, N. A., Biomedical applications of layer-by-layer assembly: from biomimetics to tissue engineering. *Adv. Mater.* **2006,** *18*, 3203.

(37) Morton, S. W.; Poon, Z.; Hammond, P. T., The architecture and biological performance of drug-loaded LbL nanoparticles. *Biomaterials* **2013,** *34*, 5328-5335.

(38) Macdonald, M. L.; Rodriguez, N. M.; Shah, N. J.; Hammond, P. T., Characterization of tunable FGF-2 releasing polyelectrolyte multilayers. *Biomacromolecules* **2010,** *11*, 2053-2059.

(39) Zhuk, I.; Jariwala, F.; Attygalle, A. B.; Wu, Y.; Libera, M. R.; Sukhishvili, S. A., Self-defensive layer-by-layer films with bacteria-triggered antibiotic release. *ACS Nano* **2014,** *8*, 7733-7745.

(40) Chaubaroux, C.; Vrana, E.; Debry, C.; Schaaf, P.; Senger, B.; Voegel, J.-C.; Haikel, Y.; Ringwald, C.; Hemmerlé, J.; Lavalle, P., Collagen-based fibrillar multilayer films cross-linked by a natural agent. *Biomacromolecules* **2012,** *13*, 2128-2135.

(41) Barthes, J.; Mertz, D.; Bach, C.; Metz-Boutigue, M.-H. l. n.; Senger, B.; Voegel, J.-C.; Schaaf, P.; Lavalle, P., Stretch-induced biodegradation of polyelectrolyte multilayer films for drug release. *Langmuir* **2012,** *28*, 13550-13554.

(42) Vogt, C.; Ball, V.; Mutterer, J.; Schaaf, P.; Voegel, J.-C.; Senger, B.; Lavalle, P., Mobility of proteins in highly hydrated polyelectrolyte multilayer films. *J. Phys. Chem. B* **2012,** *116*, 5269-5278.

(43) Dimitriadis, E. K.; Horkay, F.; Maresca, J.; Kachar, B.; Chadwick, R. S., Determination of elastic moduli of thin layers of soft material using the atomic force microscope. *Biophys. J.* **2002,** *82*, 2798-2810.

(44) Polyakov, P.; Soussen, C.; Duan, J.; Duval, J. F.; Brie, D.; Francius, G., Automated force volume image processing for biological samples. *PLoS One* **2011,** *6*, e18887.

(45) García-Nieto, S.; Johal, R. K.; Shakesheff, K. M.; Emara, M.; Royer, P.-J.; Chau, D. Y.; Shakib, F.; Ghaemmaghami, A. M., Laminin and fibronectin treatment leads to generation of dendritic cells with superior endocytic capacity. *PLoS one* **2010,** *5*, e10123.

(46) Picart, C.; Mutterer, J.; Richert, L.; Luo, Y.; Prestwich, G.; Schaaf, P.; Voegel, J.-C.; Lavalle, P., Molecular basis for the explanation of the exponential growth of polyelectrolyte multilayers. *Proc. Natl. Acad. Sci. USA* **2002,** *99*, 12531-12535.

(47) Jourdainne, L.; Lecuyer, S.; Arntz, Y.; Picart, C.; Schaaf, P.; Senger, B.; Voegel, J.-C.; Lavalle, P.; Charitat, T., Dynamics of poly (L-lysine) in hyaluronic acid/poly (L-lysine)

multilayer films studied by fluorescence recovery after pattern photobleaching. *Langmuir* **2008,** *24*, 7842-7847.

(48) Vodouhê, C.; Schmittbuhl, M.; Boulmedais, F.; Bagnard, D.; Vautier, D.; Schaaf, P.; Egles, C.; Voegel, J.-C.; Ogier, J., Effect of functionalization of multilayered polyelectrolyte films on motoneuron growth. *Biomaterials* **2005,** *26*, 545-554.

(49) Pulendran, B.; Artis, D., New Paradigms in Type 2 Immunity. *Science* **2012,** *337*, 431-435.

Table of Contents Graphic